Eur. Phys. J. C (2022) 82:30
https://doi.org/10.1140/epjc/s10052-021-09975-z

THE EUROPEAN PHYSICAL JOURNAL C

Regular Article - Theoretical Physics

Impact of $b \to s\ell\ell$ anomalies on rare charm decays in non-universal Z' models

Ashutosh Kumar Alok[1,a], **Neetu Raj Singh Chundawat**[1,b], **Dinesh Kumar**[2,c]

[1] Indian Institute of Technology Jodhpur, Jodhpur 342037, India
[2] Department of Physics, University of Rajasthan, Jaipur 302004, India

Received: 6 November 2021 / Accepted: 24 December 2021 / Published online: 11 January 2022

Abstract In this work, we study the impact of $b \to s\ell\ell$, $B_s - \bar{B_s}$ mixing and neutrino trident measurements on observables in decays induced by $c \to u$ transition in the context of a non-universal Z' model which generates $C_9^{\rm NP} < 0$ and $C_9^{\rm NP} = -C_{10}^{\rm NP}$ new physics scenarios at the tree level. We inspect the effects on $D^0 \to \pi^0\nu\bar{\nu}$, $D^+ \to \pi^+\nu\bar{\nu}$ and $B_c \to B^+\nu\bar{\nu}$ decays which are induced by the quark level transition $c \to u\nu\bar{\nu}$. The fact that the branching ratios of these decays are negligible in the standard model (SM) and the long distance effects are relatively smaller in comparison to their charged dileptons counterparts, they are considered to provide genuine null-tests of SM. Therefore the observation of these modes at the level of current as well as planned experimental sensitivities would imply unambiguous signature of new physics. Using the constraints on Z' couplings coming from a combined fit to $b \to s\ell\ell$, ΔM_s and neutrino trident data, we find that any meaningful enhancement over the SM value is ruled out in the considered framework. The same is true for $D - \bar{D}$ mixing observable ΔM_D along with $D^0 \to \mu^+\mu^-$ and $D^+ \to \pi^+\mu^+\mu^-$ decay modes which are induced through $c \to u\mu^+\mu^-$ transition.

1 Introduction

The currently running experiments at the LHC have provided several engrossing indirect hints of physics beyond the standard model (SM) of electroweak interactions. Many such signatures of new physics are in observables related to the decays induced by the quark level transition $b \to s\,\ell^+\,\ell^-$ $(l = e,\ \mu)$ [1]. The most interesting discrepancies are related to lepton flavour universality (LFU) violation in decays $B \to (K,\ K^*)\,l^+\,l^-$ as within the SM, the coupling of leptons of gauge bosons are flavour independent. The measurements of LFU testing ratios $R_K \equiv \Gamma(B^+ \to K^+\mu^+\mu^-)/\Gamma(B^+ \to K^+e^+e^-)$ [2] and $R_{K^*} \equiv \Gamma(B^0 \to K^{*0}\mu^+\mu^-)/\Gamma(B^0 \to K^{*0}e^+e^-)$ [3] disagree with the SM prediction which is very close to unity [4–6], with small corrections due to the muon–electron mass difference, at the level of 3.1 and 2.5σ, respectively. Very recently such ratios were measured in $B^0 \to K_S^0 l^+l^-$ and $B^+ \to K^{*+}\ell^+\ell^-$ decay modes by the LHCb collaboration using data set corresponding to an integrated luminosity of 9 fb^{-1} [7]. These measurements have relatively large uncertainties and they are consistent with the SM value at 1.5 and 1.4σ, respectively. These discrepancies can be attributed to new physics in muon or/and electron sector.

There is another class of discrepancies that can be imputed to new physics only in the muon sector. These are in angular observables constructed from kinematical distribution of differential decay widths of $B \to K^*\,\mu^+\,\mu^-$ and $B_s \to \phi\,\mu^+\,\mu^-$ decays. A series of measurements from different experiments at the LHC along with the Belle experiment have reported deviations from their SM predictions of the angular observable P_5' in $B \to K^*\,\mu^+\,\mu^-$ decay at the level of 3σ [8–10]. In addition, the measured value of the branching ratio of $B_s \to \phi\,\mu^+\,\mu^-$ decay shows tension with the SM prediction at the level of 3.5σ [11].

The piling up of these disparateness with the SM can be considered as signals of new physics. The Lorentz structure of this possible new physics can be determined by a model-independent analysis within the framework of effective field theory (EFT) where the new physics effects are incorporated by adding new operators O_i to the SM effective Hamiltonian. The contributions of heavy new particles are integrated out and decoded in the Wilson coefficients (WCs) C_i of the operators O_i. A global analyses of all relevant data in $b \to s\,\ell^+\,\ell^-$ sector have been performed by several groups, see for e.g. [12–20]. These analyses differ mainly in the treatment of hadronic uncertainties and the sta-

[a] e-mail: akalok@iitj.ac.in
[b] e-mail: chundawat.1@iitj.ac.in
[c] e-mail: dinesh@uniraj.ac.in (corresponding author)

tistical approach. Irrespective of the adopted methodology in these analyses, new physics scenarios with non-zero muonic WCs corresponding to vector/axial-vector operators are statistically favoured.

The global analyses of $b \to s\,\ell^+\,\ell^-$ data suggest various new physics solutions. Some of these solutions are preferred over the SM with a very high significance. For e.g., considering one new physics operator or two related operators at a time and assuming new physics only in the muon sector, the $O_9 \equiv (\bar{s}\gamma^\mu P_L b)(\overline{\mu}\gamma_\mu \mu)$ operator as well as a combination of O_9 and $O_{10} \equiv (\bar{s}\gamma^\mu P_L b)(\overline{\mu}\gamma_\mu\gamma_5 \mu)$ with $C_9^{NP} = -\,C_{10}^{NP}$ can account for all $b \to s\,\ell^+\,\ell^-$ data. These model independent solutions can be realized in several new physics models. One such simplified model is Z' with non-universal couplings which generates $b \to s\,\mu^+\,\mu^-$ decay mode at the tree level, see for e.g. [21–36]. Various versions of these models are widely studied in the context of B-anomalies. However, the Z' boson can also contribute to other sectors. The muon coupling to Z' is constrained by $b \to s$ and neutrino trident data and hence it is possible to look for implications of such couplings in other sector as well. Such a correlation in $b \to d$ sector was studied in [37].

In this work we study implications of current $b \to s$ and neutrino trident data on several observables in the charm sector in the context of Z' models. In particular we study decays induced by the quark level transition $c \to u\nu\bar{\nu}$ and $c \to u\mu^+\mu^-$. These rare decays provide unique opportunity for probing new physics in the up quark sector. The SM symmetries are utilized to define null-test observables with small theoretical uncertainties in these semi-leptonic decays which are usually dominated by vector resonances [38]. Therefore it would be interesting to investigate the impact of possible new physics in $b \to s$ sector on charm decays which can play complementary role in understanding the nature and origin of new physics apparent in the down sector. The theoretical potential embedded in the charm sector can be complemented and utilized by the several ongoing and planned experimental facilities such as LHCb [39], Belle II [40], BES III [41], the FCC-ee [42] and Super Charm-Tau factory [43].

The paper is organized as follows. In Sect. 2, we introduce the Z' model considered in this work along with its contributions to the effective Hamiltonian of $b \to s$ and $c \to u$ processes. In the next section we discuss observables which provide useful constraints on Z' couplings relevant for the $b \to s$ sector. We also provide the fit results. Using the constraints obtained on new physics couplings, in Sect. 4, we provide predictions for several observables in the charm sector. We also show correlations between potential observables in charm and $b \to s\mu^+\mu^-$ sectors. Finally, the conclusions of this work are illustrated in Sect. 5.

2 The non-universal Z' model

We consider a non-universal Z' model where the Z' boson is associated with an additional $U(1)'$ symmetry. In this model, the $b \to s\,\mu^+\,\mu^-$ transition is generated at the tree level. The Z' boson couples to both left and right-handed muons but not to leptons of other generations. Further, the couplings to both left and right-handed quarks are allowed. However, in order to avoid contribution of new chirality flipped operators to flavour changing neutral current (FCNC) decays, the couplings to right-handed quarks are assumed to be flavour-diagonal [44,45]. As we are interested in $b \to s$ processes, the change in the Lagrangian density due to the addition of this heavy Z' boson can be written as

$$\Delta\mathscr{L}_{Z'} = J^\alpha Z'_\alpha, \tag{1}$$

where

$$J^\alpha \supset g_L^{\mu\mu}\,\bar{L}\gamma^\alpha P_L L + g_R^{\mu\mu}\,\bar{\mu}\gamma^\alpha P_R\,\mu + g_L^{bs}\,\bar{Q}_2\gamma^\alpha P_L Q_3 + h.c., \tag{2}$$

where $g_{L(R)}^{\mu\mu}$ are the left-handed (right-handed) couplings of the Z' boson to muons, and g_L^{bs} to quarks. The right handed quark coupling, g_R^{bs}, cannot contribute to the $b \to s$ processes as these couplings are assumed to be flavour diagonal. Further, $P_{L(R)} = (1 \mp \gamma_5)/2$, Q_i is the i^{th} generation of quark doublet, and $L = (\nu_\mu, \mu)^T$ is the second generation doublet.

After integrating out the heavy Z', we get the effective four-fermion Hamiltonian which apart from contributing to $b \to s\,\mu^+\,\mu^-$ transition, also induces $b \to s\,\nu\,\bar{\nu}$ and $c \to u$ transitions. The relevant terms in the effective Hamiltonian is given by

$$\begin{aligned}
\mathscr{H}_{\text{eff}}^{Z'} = \frac{1}{2M_{Z'}^2} J_\alpha J^\alpha \supset\; & \frac{g_L^{bs}}{M_{Z'}^2}\left(\bar{s}\gamma^\alpha P_L b\right) \\
& \times \left[\bar{\mu}\gamma_\alpha\left(g_L^{\mu\mu}P_L + g_R^{\mu\mu}P_R\right)\mu\right] \\
& + \frac{\left(g_L^{bs}\right)^2}{2M_{Z'}^2}\left(\bar{s}\gamma^\alpha P_L b\right)\left(\bar{s}\gamma_\alpha P_L b\right) \\
& + \frac{g_L^{\mu\mu}}{M_{Z'}^2}\left(\bar{\nu}_\mu\gamma_\alpha P_L \nu_\mu\right)\left[\bar{\mu}\gamma^\alpha\left(g_L^{\mu\mu}P_L + g_R^{\mu\mu}P_R\right)\mu\right] \\
& + \frac{g_L^{bs}\,g_L^{\mu\mu}}{M_{Z'}^2}\left(\bar{s}\gamma^\alpha P_L b\right)\left(\bar{\nu}_\mu\gamma_\alpha P_L \nu_\mu\right) \\
& + \frac{h_L^{cu}}{M_{Z'}^2}\left(\bar{u}\gamma^\alpha P_L c\right)\left[\bar{\mu}\gamma_\alpha\left(g_L^{\mu\mu}P_L + g_R^{\mu\mu}P_R\right)\mu\right] \\
& + \frac{\left(h_L^{cu}\right)^2}{2M_{Z'}^2}\left(\bar{u}\gamma^\alpha P_L c\right)\left(\bar{u}\gamma_\alpha P_L c\right) \\
& + \frac{h_L^{cu}\,g_L^{\mu\mu}}{M_{Z'}^2}\left(\bar{u}\gamma^\alpha P_L c\right)\left(\bar{\nu}_\mu\gamma_\alpha P_L \nu_\mu\right),
\end{aligned} \tag{3}$$

where $h_L^{cu} = g_L^{bs} V_{us} V_{cb}^*$. The fact that the down-type quarks in the quark-doublets Q_i are taken to be in the mass-flavour diagonal basis, $u_i \to u_j$ transitions are induced by the up-type quarks in the quark doublets.

The first term in Eq. (3) induces $b \to s\mu^+\mu^-$ transition whereas the second term gives rise to B_s–$\bar{B}_s$ mixing. The third term contributes to the neutrino trident production $\nu_\mu N \to \nu_\mu N \mu^+\mu^-$ (N = nucleus). The fourth term generates $b \to s\,\nu\,\bar{\nu}$ decay whereas the remaining terms induces FCNC transitions in the up quark sector. The contribution to $c \to u\mu^+\mu^-$ and D^0-$\bar{D}^0$ in this model can be calculated through fifth and sixth terms, respectively. The seventh term corresponds to charm dineutrino decay. The product $g_L^{bs}\, g_{L,R}^{\mu\mu}$ and the individual magnitude $|g_L^{bs}|$ are constrained by the $b \to s\mu^+\mu^-$ data and B_s–$\bar{B}_s$ mixing, respectively. The constraints on individual muon couplings $g_{L,R}^{\mu\mu}$ are obtained through the measurement of the neutrino trident production. Observables in $c \to u$ sectors depend upon specific combinations of these couplings which can be determined from Eq. (3). Thus it would be interesting to see the implications of $b \to s\mu^+\mu^-$, B_s–$\bar{B}_s$ and neutrino trident data on possible new physics effects in charm decays. We now discuss contributions of Z' boson to these processes.

2.1 $b \to s$ transitions

In this subsection, we calculate the contributions of Z' boson to $b \to s$ transitions. Here we consider $b \to s\mu^+\mu^-$ and $b \to s\nu\bar{\nu}$ decays along with $B_s - \bar{B}_s$ mixing.

2.1.1 $b \to s\mu^+\mu^-$ decay

The effective Hamiltonian for $b \to s\mu^+\mu^-$ transition in the SM is given by

$$\begin{aligned}\mathscr{H}_{\rm eff}^{\rm SM} = -\frac{4G_F}{\sqrt{2}} V_{ts}^* V_{tb} \Bigg[&\sum_{i=1}^{6} C_i O_i + C_8 O_8 \\ &+ C_7 \frac{e}{16\pi^2} [\overline{q}\sigma_{\mu\nu}(m_s P_L + m_b P_R) b] F^{\mu\nu} \\ &+ C_9^{\rm SM} \frac{\alpha_{\rm em}}{4\pi} (\overline{s}\gamma^\mu P_L b)(\overline{\mu}\gamma_\mu \mu) \\ &+ C_{10}^{\rm SM} \frac{\alpha_{\rm em}}{4\pi} (\overline{s}\gamma^\mu P_L b)(\overline{\mu}\gamma_\mu\gamma_5 \mu) \Bigg]. \end{aligned} \tag{4}$$

Here G_F is the Fermi constant and V_{ij} are the Cabibbo–Kobayashi–Maskawa (CKM) matrix elements. The short distance contributions are encoded in the Wilson coefficients (WC) C_i of the four-fermi operators O_i where the scale-dependence is implicit, i.e. $C_i \equiv C_i(\mu)$ and $O_i \equiv O_i(\mu)$. The contributions of operators O_i ($i = 1, \ldots, 6, 8$) to $b \to s\mu^+\mu^-$ are included through the modifications $C_{7,9}(\mu) \to C_{7,9}^{\rm eff}(\mu, q^2)$. Here q^2 is the invariant mass-squared of the final state muon pair. The Z' boson contributes to $b \to s\mu^+\mu^-$ decay mode through the first term in Eq. (3). This contribution modifies the SM WCs $C_{9,10}^{\rm SM}$ as $C_{9,10} \to C_{9,10}^{\rm SM} + C_{9,10}^{\rm NP}$. The new contributions $C_{9,10}^{\rm NP}$ are given as

$$\begin{aligned} C_9^{\rm NP} &= -\frac{\pi}{\sqrt{2} G_F\, \alpha_{\rm em}\, V_{tb} V_{ts}^*} \frac{g_L^{bs}(g_L^{\mu\mu} + g_R^{\mu\mu})}{M_{Z'}^2}, \\ C_{10}^{\rm NP} &= \frac{\pi}{\sqrt{2} G_F\, \alpha_{\rm em}\, V_{tb} V_{ts}^*} \frac{g_L^{bs}(g_L^{\mu\mu} - g_R^{\mu\mu})}{M_{Z'}^2}. \end{aligned} \tag{5}$$

It is well known that the new physics scenario $C_9^{\rm NP} < 0$ as well as $C_9^{\rm NP} = -\,C_{10}^{\rm NP}$ provide a good fit to all $b \to s\mu^+\mu^-$ data. It is evident from Eq. (5) that these one-dimensional (1D) new physics solutions can be generated by substituting $g_L^{\mu\mu} = g_R^{\mu\mu}$ and $g_R^{\mu\mu} = 0$, respectively. In this work, we consider both scenarios. We denote $g_L^{\mu\mu} = g_R^{\mu\mu}$ and $g_R^{\mu\mu} = 0$ scenarios as Z_1 and Z_2, respectively.

2.1.2 $B_s - \bar{B}_s$ mixing

The B_s mixing is generated in the SM through the box diagrams. The dominant contribution comes from the virtual top quark in the loop. The mass difference of the two mass eigenstates, $\Delta M_s \equiv M_H^s - M_L^s$, is two times M_{12}^s, the dispersive part of the box diagrams responsible for the mixing. Within SM, M_{12}^s is given by

$$M_{12}^{s,{\rm SM}} = \frac{G_F^2 M_W^2}{12\pi^2} \left(V_{tb} V_{ts}^*\right)^2 M_{B_s} f_{B_s}^2 \widehat{B}_{B_s} \eta_B S_0(x_t), \tag{6}$$

where $x_t \equiv m_t^2/M_W^2$, $S_0(x_t)$ is the Inami–Lim function [46] and $\eta_B \approx 0.84$ encodes perturbative QCD corrections at two loop [47]. The Z' boson generates $B_s - \bar{B}_s$ mixing at the tree-level through the second term in Eq. (3) which is the same operator as in the SM. The combined contribution is written as [48]

$$\frac{\Delta M_s^{{\rm SM}+Z'}}{\Delta M_s^{\rm SM}} \approx \left| 1 + (5 \times 10^3)(g_L^{bs})^2 \right|, \tag{7}$$

for $M_{Z'} = 1$ TeV.

2.1.3 $b \to s\nu\bar{\nu}$ decay

Like $b \to s l^+ l^-$ transition, $b \to s\nu\bar{\nu}$ occurs via one-loop electroweak penguin or box diagrams in the SM. However $b \to s\nu\bar{\nu}$ decay rates are predicted with relatively smaller theoretical uncertainties in comparison to the corresponding $b \to s l^+ l^-$ decay modes. This is mainly due to the absence of the long-distance electromagnetic interactions. The effective

Hamiltonian for $b \to s\nu\bar{\nu}$ transition is given by [49]

$$H_{\rm eff} = -\frac{\sqrt{2}G_F\,\alpha_{\rm em}}{\pi} V_{tb}V_{ts}^* \sum_\ell C_L^\ell \times (\bar{s}\gamma_\mu P_L b)(\bar{\nu}_\ell \gamma^\mu P_L \nu_\ell)\,. \tag{8}$$

Here $C_L^\ell = C_L^{\rm SM} + C_\nu^{\ell\ell}({\rm NP})$. The SM WC is $C_L^{\rm SM} = -X_t/s_W^2$, where $s_W \equiv \sin\theta_W$ and $X_t = 1.469 \pm 0.017$. The NP contribution $C_\nu^{\mu\mu}({\rm NP})$ in the Z' model is given by

$$C_\nu^{\mu\mu}({\rm NP}) = -\frac{\pi}{\sqrt{2}G_F\,\alpha_{\rm em}V_{tb}V_{ts}^*}\frac{g_L^{bs}\,g_L^{\mu\mu}}{M_{Z'}^2}. \tag{9}$$

2.2 Neutrino trident production

Due to $SU(2)_L$ invariance, the Z' also couples to the left-handed neutrinos. This leads to the neutrino trident production, $\nu_\mu N \to \nu_\mu N \mu^+\mu^-$. The the third term in Eq. (3) modifies the cross section σ for neutrino trident production as [50]

$$R_\nu = \frac{\sigma}{\sigma_{\rm SM}} = \frac{1}{1+(1+4s_W^2)^2}\left[\left(1+\frac{v^2 g_L^{\mu\mu}(g_L^{\mu\mu}-g_R^{\mu\mu})}{M_{Z'}^2}\right)^2 + \left(1+4s_W^2+\frac{v^2 g_L^{\mu\mu}(g_L^{\mu\mu}+g_R^{\mu\mu})}{M_{Z'}^2}\right)^2\right], \tag{10}$$

where $v = 246$ GeV and $s_W = \sin\theta_W$.

2.3 $c \to u$ transitions

The Z' contributes to $c \to u$ transition through fifth, sixth and seventh terms in Eq. (3). These terms induce $c \to u\mu^+\mu^-$ decay, D-$\bar{D}$ mixing and $c \to u\nu\bar{\nu}$ transition, respectively.

2.3.1 $c \to u\mu^+\mu^-$ decay

The $c \to u\mu^+\mu^-$ process in the SM can be described by the following effective Hamiltonian at the $\mu_c = m_c$ scale [51–58]

$$\mathscr{H}_{\rm eff}^{\rm SM}(c \to u\mu^+\mu^-) = (V_{ud}V_{cd}^*)\,\mathscr{H}^d + (V_{us}V_{cs}^*)\,\mathscr{H}^s + (V_{ub}V_{cb}^*)\,\mathscr{H}^{\rm peng}, \tag{11}$$

where the three contributions correspond to diagram with intermediate quarks d, s, b. It is customary to include the contributions of the states heavier than the charm quark in $\mathscr{H}^{\rm peng}$ as

$$\mathscr{H}^{\rm peng} = -\frac{4G_F}{\sqrt{2}}\sum_{i=3,\ldots,10} C_i^{cu}\,O_i. \tag{12}$$

The following operators appearing in the above effective Hamiltonian are in particular sensitive to new physics effects

$$O_7 = \frac{em_c}{4\pi^2}\left(\bar{u}\sigma_{\mu\nu}P_R c\right)F^{\mu\nu}, \tag{13}$$

$$O_9 = \frac{\alpha_{\rm em}}{4\pi}(\bar{u}\gamma^\mu P_L c)(\bar{\mu}\gamma_\mu\mu), \tag{14}$$

$$O_{10} = \frac{\alpha_{\rm em}}{4\pi}(\bar{u}\gamma^\mu P_L c)(\bar{\mu}\gamma_\mu\gamma_5\mu). \tag{15}$$

The only non-vanishing WCs in the SM are $C_{7,9}^{cu}$. Their values are determined mainly through the effects of QCD renormalization. The value of $C_7^{cu}(m_c)$ determined by two loop mixing with current-current operators is $V_{ub}V_{cb}^* C_7^{cu} = V_{us}V_{cs}^*$ $(0.007 + 0.020i)(1 \pm 0.2)$ [51,59]. After inclusion of renormalization group running effects, the value of $C_9^{cu}(m_c)$ turns out to be small [53]. On the other hand, as the renormalization group running does not affect O_{10}, the WC $C_{10}^{cu}(m_c)$ is negligibly small [60]. As $C_{10}^{cu} \approx 0$, the effects of $V-A$ structure of the SM are switched off at the charm scale. This feature makes FCNC charm decays distinct from that of the corresponding B and K decays.

The Z' boson contributes to $c \to u\mu^+\mu^-$ decay through the fifth term in Eq. (3). This contribution modifies the SM WCs $C_{9,10}^{cu}$ as $C_{9,10}^{cu,{\rm tot}} \to C_{9,10}^{cu} + C_{9,10}^{cu,Z'}$. The new contributions $C_{9,10}^{cu,Z'}$ are given by

$$C_9^{cu,Z'} = -\frac{\pi}{\sqrt{2}G_F\,\alpha_{\rm em}V_{ub}V_{cb}^*}\frac{h_L^{cu}(g_L^{\mu\mu}+g_R^{\mu\mu})}{M_{Z'}^2},$$
$$C_{10}^{cu,Z'} = \frac{\pi}{\sqrt{2}G_F\,\alpha_{\rm em}V_{ub}V_{cb}^*}\frac{h_L^{cu}(g_L^{\mu\mu}-g_R^{\mu\mu})}{M_{Z'}^2}. \tag{16}$$

For Z_1 (Z_2) model, $g_L^{\mu\mu} = g_R^{\mu\mu}$ ($g_R^{\mu\mu} = 0$).

2.3.2 D-$\bar{D}$ mixing

In the SM, D^0–$\bar{D}^0$ mixing is induced by the box diagrams with d, s and b quarks in the loop. Due to a strong GIM cancellation, the short-distance contribution is extremely small, $\Delta M_D = O(10^{-4})\,{\rm ps}^{-1}$. Therefore the short-distance contribution cannot explain the measured value of ΔM_D which is $(0.95^{+0.41}_{-0.44}) \times 10^{-2}\,{\rm ps}^{-1}$ [61]. In particular, the contribution due to b-quark is highly suppressed, $O(\lambda^8)$. The fact that D^0-$\bar{D}^0$ mixing is dominated by the d- and s-quarks, there can be large long-distance contributions, for which there are no reliable estimates at present [62,63]. As long-distance contributions are unknown, in our analysis we focus on the short-distance contributions to the D^0-$\bar{D}^0$ mixing parameter ΔM_D.

In Z' model, D^0-$\bar{D}^0$ mixing is induced at the tree level and hence expected to provide a much larger contribution in comparison to the short-distance SM contribution. ΔM_D

generated by the sixth term in Eq. (3) is given by

$$\Delta M_D = \frac{f_D^2\, m_D\, B_D\, r(m_c, M_{Z'})}{3M_{Z'}^2} |(h_L^{cu})^2|, \tag{17}$$

where $f_D = 212.0 \pm 0.7$ MeV [64], $B_D = 0.757 \pm 0.027 \pm 0.004$ [65] and the RG factor $r(m_c, M_{Z'}) = 0.72$ for $M_{Z'} = 1$ TeV [66].

2.3.3 $c \to u\nu\bar{\nu}$ decay

Within the SM, the $c \to u\nu\bar{\nu}$ transition is induced by box and Z-penguin diagrams. The corresponding short-distance effective Hamiltonian is given by [63]

$$\mathscr{H}_{\rm eff}^{\rm SM} = \sum_{\ell=e,\mu,\tau} C_\ell^{\rm SM} \left(\bar{u}\gamma^\mu(1-\gamma_5)c\right)\left(\bar{\nu}_\ell\gamma_\mu(1-\gamma_5)\nu_\ell\right), \tag{18}$$

where

$$C_\ell^{\rm SM} = -\frac{G_F}{\sqrt{2}}\frac{\alpha_{\rm em}}{2\pi\,\sin^2\theta_W}\sum_{q=d,s,b}\lambda_q X^\ell(x_q). \tag{19}$$

Here $\lambda_q = V_{uq}V_{cq}^*$ and the structure functions are defined by $X^\ell(x_q) = \bar{D}(x_q,\, y_\ell)/2$, where $\bar{D}(x_q,\, y_\ell)$ is given as [46]

$$\begin{aligned}
&\bar{D}(x_q,\, y_\ell)\\
&= \frac{1}{8}\frac{x_q\, y_\ell}{x_q - y_\ell}\left(\frac{y_\ell - 4}{y_\ell - 1}\right)^2 \ln y_\ell + \frac{x_q}{4}\\
&\quad + \frac{x_q}{8}\left[\frac{x_q}{y_\ell - x_q}\left(\frac{x_q - 4}{x_q - 1}\right)^2 + 1 + \frac{3}{(x_q-1)^2}\right]\ln x_q\\
&\quad - \frac{3}{8}\left(1 + \frac{3}{y_\ell - 1}\right)\frac{x_q}{x_q - 1},
\end{aligned} \tag{20}$$

with $x_q = m_q^2/M_W^2$ and $y_l = m_l^2/M_W^2$.

The Z' contributes to $c \to u\nu\bar{\nu}$ transition through the seventh term in Eq. (3). This contribution modifies the WC as $C_\ell \to C_\ell^{\rm SM} + \mathscr{C}_\mu^{\nu\nu}$, where

$$\mathscr{C}_\mu^{\nu\nu} = \frac{h_L^{cu}\, g_L^{\mu\mu}}{4M_{Z'}^2}. \tag{21}$$

3 Constraints on NP couplings

In the literature there are several works where the rare charm decays have been studied in the context of Z' models. However, in most of these works, the constraints coming from $b \to s\,\mu^+\,\mu^-$ sector were not considered. To emphasize the fact that $b \to s\,\mu^+\,\mu^-$ sector can provide valuable constraints on the allowed new physics parameter space and hence restrict large new physics contributions to several observables in the up sector, we perform four types of fit:

- F1: only $b \to s\nu\bar{\nu}$ data,
- F2: $b \to s\nu\bar{\nu}$ data and $B_s - \bar{B}_s$ mixing,
- F3: $b \to s\nu\bar{\nu}$ data, $B_s - \bar{B}_s$ mixing and neutrino trident,
- F4: $b \to s\nu\bar{\nu}$ data, $B_s - \bar{B}_s$ mixing, neutrino trident and $b \to s\,\mu^+\,\mu^-$ data.

In the following, we discuss all observables used in the fit. These observables can be classified into following four sectors:

$b \to s\nu\bar{\nu}$ sector: The quark level transition $b \to s\nu\bar{\nu}$ induces exclusive semi-leptonic decays $B \to K^{(*)}\nu\bar{\nu}$. The experimental measurement of $b \to s\nu\bar{\nu}$ decay modes are challenging due to the presence of two final state neutrinos and require clean environment facilities such as e^+e^- colliders. At present, we only have upper bound in $b \to s\nu\bar{\nu}$ sector coming from Belle [67,68] and BaBar [69] experiments. The current upper limits for $B \to K^{(*)}\nu\bar{\nu}$ decays at 90% C.L. are [67–69]

$$\begin{aligned}
B(B^0 \to K^0\nu\bar{\nu}) &< 2.6 \times 10^{-5}\,,\\
B(B^0 \to K^{*0}\nu\bar{\nu}) &< 1.8 \times 10^{-5}\,,\\
B(B^+ \to K^+\nu\bar{\nu}) &< 1.6 \times 10^{-5}\,,\\
B(B^+ \to K^{*+}\nu\bar{\nu}) &< 4.0 \times 10^{-5}\,.
\end{aligned} \tag{22}$$

These upper bounds are a factor of two to five above the SM predictions. With 50 ab^{-1} of data, Belle-II experiment is expected to observe these decay modes to an accuracy of 10% on the branching ratio [40,70]. In order to include these observables in the fit, we convert the above upper limits to a branching ratio as (0.5 UB $\pm$ 0.625 UB) where UB is the experimental upper bound at 90% C.L. The χ^2 is then written as

$$\begin{aligned}
\chi^2_{b\to s\nu\bar{\nu}} = &\left(\frac{B(B^0 \to K^0\nu\bar{\nu}) - 1.3\times 10^{-5}}{0.81\times 10^{-5}}\right)^2\\
&+\left(\frac{B(B^0 \to K^{*0}\nu\bar{\nu}) - 0.9\times 10^{-5}}{0.56\times 10^{-5}}\right)^2\\
&+\left(\frac{B(B^+ \to K^{+}\nu\bar{\nu}) - 0.8\times 10^{-5}}{0.5\times 10^{-5}}\right)^2\\
&+\left(\frac{B(B^+ \to K^{*+}\nu\bar{\nu}) - 2.0\times 10^{-5}}{1.25\times 10^{-5}}\right)^2,
\end{aligned} \tag{23}$$

where the theoretical predictions for $B \to K^{(*)}\nu\nu$ branching ratios are obtained using `Flavio` [71]. We do not use constraints from the branching ratio of $B_s \to \phi\nu\bar{\nu}$ as it is much weaker than $B \to K^{(*)}\nu\bar{\nu}$ decay modes.

$B_s - \bar{B}_s$ sector: Here we consider constraints coming from the mass difference ΔM_s. Using Eq. (7), the constraints on

Table 1 Various inputs used in the fits

Observable	Value	Observable	Value
G_F	1.16637×10^{-5} [61]	$B(B^0 \to K^0 \nu\bar{\nu})$	2.6×10^{-5} [67]
$\alpha_e(m_Z)$	1/127.9 [61]	$B(B^0 \to K^{*0} \nu\bar{\nu})$	1.8×10^{-5} [67]
$\sin^2\theta_W$	0.23121 [61]	$B(B^+ \to K^+ \nu\bar{\nu})$	1.6×10^{-5} [69]
λ	0.22650 ± 0.00048 [61]	$B(B^+ \to K^{*+} \nu\bar{\nu})$	4.0×10^{-5} [68]
A	$0.790^{+0.017}_{-0.012}$ [61]	$\Delta M_s^{\rm SM}/\Delta M_s^{\rm Exp}$	$1.04^{+0.04}_{-0.07}$ [48]
$\bar{\rho}$	$0.141^{+0.016}_{-0.017}$ [61]	R_ν	0.82 ± 0.28 [73,74]
$\bar{\eta}$	0.357 ± 0.011 [61]	$C_9^{\rm NP}$	-1.01 ± 0.15 [14]
M_W	80.385 [61]	$C_9^{\rm NP} = -C_{10}^{\rm NP}$	-0.49 ± 0.07 [14]
m_t	162.5 [61]		

g_L^{bs} can be translated in the following form

$$(g_L^{bs})^2 = (7.69 \pm 12.94) \times 10^{-6}. \tag{24}$$

Here we used the value of $\Delta M_s^{\rm SM}/\Delta M_s^{\rm Exp}$ given in Table 1. Hence the contribution of ΔM_s to χ^2 is

$$\chi^2_{\Delta M_s} = \left(\frac{(g_L^{bs})^2 - 7.69 \times 10^{-6}}{12.94 \times 10^{-6}}\right)^2. \tag{25}$$

Neutrino trident: The contribution to the total χ^2 coming from neutrino trident production is

$$\chi^2_{\rm trident} = \left(\frac{R_\nu - 0.82}{0.28}\right)^2. \tag{26}$$

The theoretical expression of R_ν is given in Eq. (10) whereas the experimental value is taken from Table 1.

$b \to s\,\mu^+\,\mu^-$ *sector:* A fit to all $b \to s\,\mu^+\,\mu^-$ data leads to constraints on $C_9^{\rm NP}$ and $C_9^{\rm NP} = -\,C_{10}^{\rm NP}$ scenarios as given in Table 1. The fit value for $C_9^{\rm NP}$ ($C_9^{\rm NP} = -\,C_{10}^{\rm NP}$) provides constraints on Z_1 (Z_2) model. Using the fit values and other inputs from Table I along with Eq. (5), we get

$$(g_L^{bs}\, g_L^{\mu\mu})_{Z_1} = (-8.36 \pm 1.24) \times 10^{-4}, \tag{27}$$
$$(g_L^{bs}\, g_L^{\mu\mu})_{Z_2} = (-8.11 \pm 1.16) \times 10^{-4}. \tag{28}$$

We use above constraints on $(g_L^{bs}\, g_L^{\mu\mu})$ in the fit. Hence the χ^2 function can be written as

$$\chi^2_{b\to s\mu\mu,\,Z_1} = \left(\frac{(g_L^{bs}\, g_L^{\mu\mu}) - (-8.36 \times 10^{-4})}{1.24 \times 10^{-4}}\right)^2, \tag{29}$$

$$\chi^2_{b\to s\mu\mu,\,Z_2} = \left(\frac{(g_L^{bs}\, g_L^{\mu\mu}) - (-8.11 \times 10^{-4}}{1.16 \times 10^{-4}}\right)^2. \tag{30}$$

Therefore, the χ^2 for fits F1-F4 can be written as

$$\chi^2_{\rm F1} = \chi^2_{b\to s\nu\bar{\nu}}, \tag{31}$$

$$\chi^2_{\rm F2} = \chi^2_{b\to s\nu\bar{\nu}} + \chi^2_{\Delta M_s}, \tag{32}$$

$$\chi^2_{\rm F3} = \chi^2_{b\to s\nu\bar{\nu}} + \chi^2_{\Delta M_s} + \chi^2_{\rm trident}, \tag{33}$$

$$\chi^2_{\rm F4} = \chi^2_{b\to s\nu\bar{\nu}} + \chi^2_{\Delta M_s} + \chi^2_{\rm trident} + \chi^2_{b\to s\mu\mu}. \tag{34}$$

The χ^2 fit is performed using the CERN minimization code `MINUIT` [72]. The mass of Z' is assumed to be 1 TeV in the fits.

For F1 fit, χ^2 is a function of the product $(g_L^{bs}\, g_L^{\mu\mu})$. The fit result is

$$(g_L^{bs}\, g_L^{\mu\mu}) = -0.0047 \pm 0.0051. \tag{35}$$

The results for F2, F3 and F4 fits for Z_1 and Z_2 models are presented in Fig. 1. It is obvious from the figure that if we only include constraints coming from $b \to s\nu\bar{\nu}$ and ΔM_s, a relatively large parameter space is allowed. Therefore while correlating $c \to u$ decays, in particular $c \to u\nu\bar{\nu}$, with $b \to s$ sector if only these constraints are considered, a possibility of large new physics effects may survive.

However, the parameter space shrinks after including neutrino trident in the fit. Finally, after including $b \to s\mu^+\mu^-$ constraints, the allowed range of new physics couplings reduces considerably. Therefore it will be interesting to see whether any useful new physics effects in charm sector, particularly decays induced by $c \to u\nu\bar{\nu}$ and $c \to u\mu^+\mu^-$ transitions, is allowed by the current $b \to s$ and neutrino trident data.

4 Semi-leptonic charm decays and mixing

Rare or forbidden decays of charm mesons provide a unique channel to probe new physics in the up-type quark sector [38]. This is complementary to new physics searches in the first and third generations of quarks as well as in the down-quark sectors. The fact that the charm quark is not as heavy as bottom, the application of heavy quark effective theory is not as useful as it is for the B-meson sector. Also the mass of

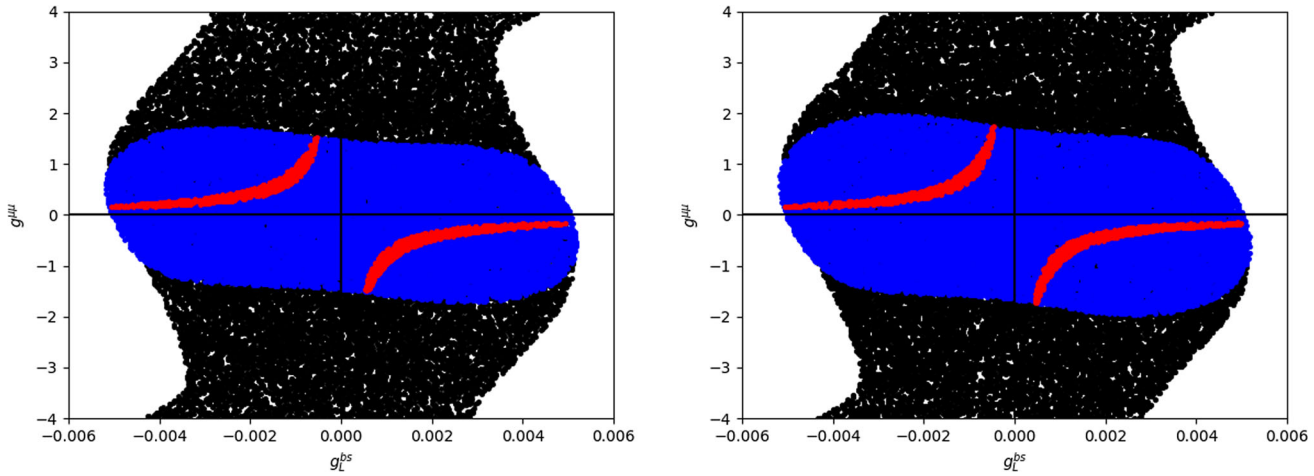

Fig. 1 The left and right panels depict 1σ-favoured parameter space of $(g_L^{bs},\ g_L^{\mu\mu})$ couplings for Z_1 and Z_2 models, respectively. The black, blue and red regions show allowed parameter space corresponding to F2, F3 and F4 fits, respectively. The allowed regions correspond to $M_{Z'} = 1$ TeV

charm quark is not small enough to be considered as a light quark. Therefore predictions in the charm sector are usually dominated by the long-distance effects. Within the SM, the short-distance contributions to the purely leptonic and semi-leptonic charm decays along with $D - \bar{D}$ mixing are highly suppressed, in fact almost negligible, owing to GIM cancellation and CKM suppression. Probing new physics then becomes a challenging task as an unambiguous signal would require enhancements above the level of long-distance contributions.

In the following subsections we discuss the impact of measurements in B meson sector on rare FCNC processes induced by the $c \to u$ transition in the context of non-universal Z' models. We consider decays induced by $c \to u\nu\bar{\nu}$ and $c \to u\mu^+\mu^-$ transitions along with $D - \bar{D}$ mixing. The primary motive is to identify observable(s) for which the current $b \to s$ data allows short-distance contributions above the long-distance contributions.

4.1 Branching ratio of dineutrino charm decays

The new physics searches can be exquisitely performed using the null-tests of the SM. In the up-sector, $c \to u$ transitions provide such null tests due to strong CKM suppression. In this regard, the decays induced by the quark level transition $c \to u\nu\bar{\nu}$ are particularly interesting as the long-distance effects are relatively smaller in comparison to their charged dileptons counterparts. Hence in $c \to u$ sector, dineutrino modes can be considered to provide genuine null-tests of SM [38,75–78]. The $c \to u\nu\bar{\nu}$ transition induces several exclusive decay modes such as $D^+ \to \pi^+\nu\bar{\nu}$, $D^0 \to \pi^0\nu\bar{\nu}$ and $B_c^+ \to B^+\nu\bar{\nu}$. Any observation of these decays at the level of current experimental sensitivity can be considered as unambiguous signature of beyond SM physics.

On the experimental front, currently there are no experimental upper limits on any of the semi-leptonic decays included by $c \to u\nu\bar{\nu}$ transition. We only have upper limits obtained using the $SU(2)_L$ invariance and bounds on the charged lepton decay modes which allow branching ratios to be as high as a few times 10^{-5} [75]. These limits can go down if charged leptons bounds are improved. Owing to the clean hadronic environments, the e^-e^- colliders such as Belle II [40], BES III [41] as well as the future colliders, for instance FCC-ee [42] are well suited for the studies related to the dineurino decay modes. For efficiencies of a permille or better, D decay modes can be observed at the Belle II and FCC-ee experiments provided new physics enhances their branching ratios up to a level of $O(10^{-6})$–$O(10^{-8})$ [76].

In this section we analyse $D^0 \to \pi^0\nu\bar{\nu}$, $D^+ \to \pi^+\nu\bar{\nu}$ and $B_c^+ \to B^+\nu\bar{\nu}$ decays in the context of non-universal Z' models. The differential branching ratio of $M_1 \to M_2\nu\bar{\nu}$ mode, where $M_1 = D^0, D^+, B_c$ and $M_2 = \pi^0, \pi^+$ and B^+, respectively is given by

$$\frac{dB}{dq^2} = \frac{\tau_{M_1}\ |f_+(q^2)|^2\ \lambda^{3/2}}{32\,\pi^3\,m_{M_1}^3}|C_\ell|^2, \tag{36}$$

where q^2 denotes the invariant mass-squared of the dineutrinos, $\lambda \equiv \lambda(m_{M_1}^2, m_{M_2}^2, q^2)$ is the Kallen function defined as $\lambda(x, y, z) = (x + y + z)^2 - 4(xy + yz + zx)$ and τ_{M_1} is the lifetime of the M_1 meson. The $M_1 \to M_2$ form-factors are defined as

$$\begin{aligned}\langle M_2(p')|\bar{u}\gamma_\mu c|M_1(p)\rangle &= f_+(q^2)\left(p_\mu + p'_\mu - \frac{m_{M_1}^2 - m_{M_2}^2}{q^2}q_\mu\right)\\ &+ f_0(q^2)\frac{m_{M_1}^2 - m_{M_2}^2}{q^2}q_\mu.\end{aligned} \tag{37}$$

Table 2 1σ upper limit on the branching ratios obtained by using constraints on Z' couplings for Z_1 model

Constraints	$C_\ell^{\max}$	$B(D^0 \to \pi^0 \nu\bar{\nu})$	$B(D^+ \to \pi^+ \nu\bar{\nu})$	$B(B_c \to B^+ \nu\bar{\nu})$
$b \to s\nu\nu$	7.4×10^{-11}	5.6×10^{-12}	2.2×10^{-11}	4.2×10^{-12}
$b \to s\nu\nu$, ΔM_s	7.4×10^{-11}	5.6×10^{-12}	2.2×10^{-11}	4.3×10^{-12}
$b \to s\nu\nu$, ΔM_s, Neutrino trident	1.4×10^{-11}	2.1×10^{-13}	8.8×10^{-13}	1.6×10^{-13}
$b \to s\nu\nu$, ΔM_s, Neutrino trident, $b \to s\ell^+\ell^-$	2.3×10^{-12}	5.5×10^{-15}	2.2×10^{-14}	4.2×10^{-15}

The $D \to \pi$ and $B_c \to B$ form-factors are calculated within the framework of lattice QCD in refs. [79] and [80], respectively.

The integrated branching ratio is then given by

$$B(M_1 \to M_2 \nu\bar{\nu}) = \frac{\tau_{M_1} |C_\ell|^2}{32\pi^3 m_{M_1}^3} \int_{q^2_{\min}}^{q^2_{\max}} \lambda^{3/2} \left| f_+(q^2) \right|^2 dq^2. \tag{38}$$

For $D^0 \to \pi^0 \nu\bar{\nu}$ mode, $q^2_{\min} = 0$ whereas $q^2_{\max} = (m_{D^0} - m_{\pi^0})^2$. In $D^+ \to \pi^+ \nu\bar{\nu}$ decay, resonant backgrounds through τ-leptons lead to the same final state. This is removed by phase space cuts due to which $q^2_{\min}$ for $D^+ \to \pi^+ \nu\bar{\nu}$ mode is $(m_\tau^2 - m_{\pi^+}^2)(m_{D^+}^2 - m_\tau^2)/m_\tau^2 \approx 0.34\ \text{GeV}^2$. The $q^2_{\max}$ for this mode is $(m_{D^+} - m_{\pi^+})^2$. For $B_c \to B^+ \nu\bar{\nu}$ mode, $q^2_{\min} = 0$ whereas $q^2_{\max} = (m_{B_c} - m_{B^+})^2$. Using the form-factor calculations in [79,80], we get

$$B(D^0 \to \pi^0 \nu\bar{\nu}) \approx 1.0 \times 10^9 |C_\ell|^2, \tag{39}$$

$$B(D^+ \to \pi^+ \nu\bar{\nu}) \approx 4.1 \times 10^9 |C_\ell|^2, \tag{40}$$

$$B(B_c \to B^+ \nu\bar{\nu}) \approx 7.7 \times 10^8 |C_\ell|^2. \tag{41}$$

The short-distance SM predictions for the branching ratios of $D^0 \to \pi^0 \nu\bar{\nu}$ and $D^+ \to \pi^+ \nu\bar{\nu}$ are $\sim 2 \times 10^{-16}$ and $\sim 8 \times 10^{-16}$, respectively. The long-distance contributions in these decay modes are predicted to be $\sim 10^{-16}$ [52]. For $B_c \to B^+ \nu\bar{\nu}$ mode, the short-distance SM contribution is $\sim 1.5 \times 10^{-16}$ whereas the long-distance contribution is estimated to be $\sim 10^{-16}$ [77]. Therefore for unambiguous signature of new physics in these decay modes, the short-distance branching ratio should be enhanced well above 10^{-16}.

The decay mode $D^+ \to \pi^+ \nu\bar{\nu}$ in Z' models was studied in [76]. It was shown that the branching ratio of $D^+ \to \pi^+ \nu\bar{\nu}$ can be enhanced up to $\sim 10^{-6}$ which falls in the same ballpark as the model-independent upper bound. In [77], it was shown that the branching ratio of $B_c^+ \to B^+ \nu\bar{\nu}$ in the 331 model can be enhanced up to $\sim 10^{-11}$. It would be interesting to see whether such large enhancements is allowed by the current $b \to s$ and neutrino trident data in the non universal Z' model considered in this work.

Using the allowed range of Z' couplings obtained in Sec. 3, the 1σ upper limit on $B(D^0 \to \pi^0 \nu\bar{\nu})$, $B(D^+ \to \pi^+ \nu\bar{\nu})$ and $B(B_c \to B^+ \nu\bar{\nu})$ for Z_1 model are given in Table 2. It is obvious that if we only use constraints from dineutrino bottom decays, about four orders of magnitude enhancement in the branching ratio is allowed. The conclusions remain almost the same if ΔM_s is included in the fit along with $b \to s\nu\bar{\nu}$. However there is a large reduction in the allowed parameter space if constraints from neutrino trident are included. The parameter space shrinks further by additional of $b \to s\ell^+\ell^-$ data. For the combined fit F4, the branching ratios can only be enhanced up to an order of magnitude above the SM value. This is also evident from Fig. 2 which illustrates correlations between $B(D^+ \to \pi^+ \nu\bar{\nu})$ and $b \to s\mu^+\mu^-$ observables R_K, P_5' and $B(B_s \to \phi\mu^+\mu^-)$ in Z_1 model. The conclusions are almost the same for the Z_2 model. This enhancement is not useful in the sense that it is orders of magnitude smaller than the detection level for these modes in any of the currently running or planned collider facilities.

4.2 Branching ratio of dimuon charm decays

In this section we consider $D^0 \to \mu^+\mu^-$ and $D^+ \to \pi^+\mu^+\mu^-$ decays which are induced by the quark level transition $c \to u\mu^+\mu^-$. In the SM, the short-distance contributions to these decay modes are highly suppressed and the dominant contribution comes from the long-distance effects. It would be interesting to see whether the new physics contributions coming from the addition of Z' can enhance the decay rates above the long-distance contributions.

4.2.1 $D^0 \to \mu^+\mu^-$ decay

The short-distance contribution to the branching ratio of $D^0 \to \mu^+\mu^-$ decay is negligible in the SM. This is due to two fold effect:

- Within SM, only C_{10}^{cu} WC contributes and its value is negligibly small.
- $D^0 \to \mu^+\mu^-$ suffers from helicity suppression.

In the SM, the branching ratio of $D^0 \to \mu^+\mu^-$ decay is dominated by the long-distance effects in $D^0 \to \gamma^*\gamma^* \to \mu^+\mu^-$ [52,81,82]. Using the upper bound on $D^0 \to \gamma\gamma < 8.5 \times 10^{-7}$ at 90% C.L. [61], the SM branching ratio is estimated

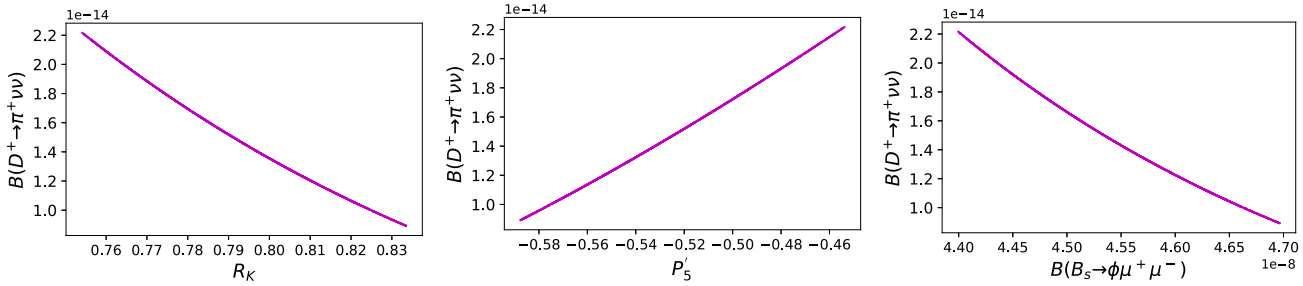

Fig. 2 Plots indicating correlations between the branching ratio of $D^+ \to \pi^+\nu\bar{\nu}$ and $b \to s\mu^+\mu^-$ observables R_K, P_5' and $B(B_s \to \phi\mu^+\mu^-)$ in Z_1 model. The correlations are almost the same for Z_2 model

to be [38,57]

$$B(D^0 \to \mu^+\mu^-)_{\rm LD} \approx 8\alpha^2 \left(\frac{m_\mu^2}{m_{D^0}^2}\right) \log^2\left(\frac{m_\mu^2}{m_{D^0}^2}\right) \times B(D^0 \to \gamma\gamma) \sim 10^{-11}. \quad (42)$$

From the experimental side, we only have an upper bound. The most stringent upper bound is reported by the LHCb experiment in 2013 which is 6.2×10^{-9} at 90% C.L. using the data-set corresponding to an integrated luminosity of 0.9 fb^{-1} [83]. Therefore the SM value of the branching ratio including the long-distance effects is well below the current experimental upper limit. Hence one can safely neglect the SM contribution while calculating the branching ration in Z' model. Under this assumption, the branching ratio is given by

$$B(D^0 \to \mu^+\mu^-)_{Z'} = \frac{\tau_{D^0} f_D^2 m_\mu^2 m_{D^0}}{32\pi M_{Z'}^4} \sqrt{1-\frac{4m_\mu^2}{m_{D^0}^2}} \times (h_L^{cu})^2 (g_L^{\mu\mu} - g_R^{\mu\mu})^2, \quad (43)$$

where $f_D = 212.0 \pm 0.7$ MeV [64] and $\tau_{D^0} = 4.101 \times 10^{-13}$ s [61]. It should be noted that $B(D^0 \to \mu^+\mu^-)_{Z'} = 0$ for Z_1 model.

Using constraints obtained on new physics couplings for Z_2 model, we find that $B(D^0 \to \mu^+\mu^-)_{Z'}$ can be as large as 5×10^{-13} for the F1 fit. For fits F2, F3 and F4, the upper bounds on $B(D^0 \to \mu^+\mu^-)_{Z'}$ are 5×10^{-13}, 2×10^{-14} and 5×10^{-16}, respectively. Thus it becomes apparent that the current $b \to s$ and neutrino trident data rules out any useful enhancement in $B(D^0 \to \mu^+\mu^-)_{Z'}$.

4.2.2 $D^+ \to \pi^+\mu^+\mu^-$ decay

The quark level transition $c \to u\mu^+\mu^-$ generates semi-leptonic decay $D^+ \to \pi^+\mu^+\mu^-$. Within SM, the short-distance contribution to the total branching ratio is highly suppressed, $O(10^{-12})$ [57]. The dominant contribution comes from vector resonances ρ, ω and ϕ, decaying to dimuon pair. The effects of these resonances are incorporated assuming naive factorization by addition of q^2-dependent terms to C_9^{cu} [57]. The contribution to the total branching ratio coming from vector resonances is $O(10^{-10})$ [84]. On the experimental front, at present we only have upper bounds. In 2013, LHCb reported following upper limits at 90% C.L. in the low- and high-q^2 bins using data corresponding to an integrated luminosity of 1.0 fb^{-1} [85]

$$B(D^+ \to \pi^+\mu^+\mu^-)_{{\rm low}-q^2} < 2.0 \times 10^{-8}, \quad (44)$$

$$B(D^+ \to \pi^+\mu^+\mu^-)_{{\rm high}-q^2} < 2.6 \times 10^{-8}. \quad (45)$$

Here low- and high-q^2 bins correspond to (0.0625, 0.276) GeV^2 and (1.56, 4.00) GeV^2, respectively.

Given the current experimental accuracy, we neglect the SM contribution. Under this assumption, the differential branching ratio in the Z' model, which generates $c \to u\mu^+\mu^-$ transition through fifth term in Eq. (3), is given by

$$\left(\frac{dB}{dq^2}\right)_{Z'} = \frac{\tau_{D^+}\lambda^{1/2}\beta_\mu}{1024\,\pi^3 m_{D^+}^3 M_{Z'}^4} \times \Big[a_1(q^2)(h_L^{cu})^2(g_L^{\mu\mu}+g_R^{\mu\mu})^2 + a_2(q^2)(h_L^{cu})^2(g_L^{\mu\mu}-g_R^{\mu\mu})^2\Big], \quad (46)$$

where λ is the Kallen function, $\beta_\mu = \sqrt{1-4m_\mu^2/q^2}$ and $\tau_{D^+} = 1.04 \times 10^{-12}$ s [61]. The functions $a_{1(2)}(q^2)$ are defined as

$$a_1(q^2) = \left(\frac{\lambda}{2} - \frac{\lambda\beta_\mu^2}{6}\right) f_+^2(q^2), \quad (47)$$

$$a_2(q^2) = a_1(q^2) + 8m_\mu^2 m_{D^+}^2 f_+^2(q^2) + 2q^2 m_\mu^2 F^2(q^2) - 4m_\mu^2\left(m_{D^+}^2 - m_{\pi^+}^2 + q^2\right) f_+(q^2)F(q^2), \quad (48)$$

with

$$F(q^2) = f_+(q^2) - \frac{m_{D^+}^2 - m_{\pi^+}^2}{q^2}\left(f_0(q^2) - f_+(q^2)\right). \quad (49)$$

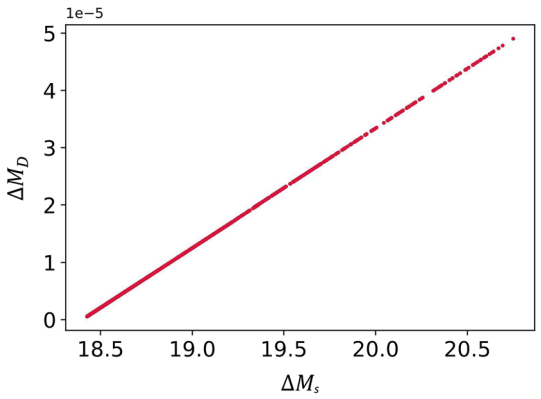

Fig. 3 Plot indicating correlations between ΔM_s and ΔM_D. The values are in the units of ps^{-1}

The $D^+ \to \pi^+$ form-factors $f_+(q^2)$ and $f_0(q^2)$ are defined in Eq. (37). The q^2 dependence of these form-factors are given in the Becirevic–Kaidalov (BK) parametrization as [86]

$$f_+(q^2) = \frac{f_+(0)}{(1-x)(1-ax)}, \tag{50}$$

$$f_0(q^2) = \frac{f_+(0)}{(1-x/b)}, \tag{51}$$

where $x \equiv q^2/m^2_{\text{pole}}$ with $m_{\text{pole}} = 1.90 \pm 0.08$ GeV, $a = 0.28 \pm 0.14$ and $b = 1.27 \pm 0.17$ are the shape parameters [57]. These shape parameters are determined by measurements of $D \to \pi l \nu$ decay spectra. The form-factor $f_+(0)$ calculated by the HPQCD collaboration is 0.67 ± 0.03 [87].

For F1, F2, F3 and F4 fits, the Z' contribution in Z_1 model to the branching ratio of $D^+ \to \pi^+\mu^+\mu^-$, $B(D^+ \to \pi^+\mu^+\mu^-)_{Z'}$, in the low-$q^2$ region are 3×10^{-12}, 3×10^{-12}, 6×10^{-14} and 3×10^{-15}, respectively. The SM short distance prediction for $B(D^+ \to \pi^+\mu^+\mu^-)$ in the low-q^2 region is 3×10^{-13}. Thus we see that if we use constraints coming from the combined fit, the new physics contribution is negligible. The same is true in the high-q^2 region. The conclusion remains unchanged for the Z_2 model.

4.3 Charm mixing

The observed value of ΔM_D is much higher than the short-distance SM value but it is in qualitative accord with the long distance SM predictions. However as no reliable estimate of the later is obtained so far, the possibility of large new physics contributions to $D - \bar{D}$ mixing is not ruled out. Here we consider such an effect in the context of Z' model. In the current framework, the contribution to ΔM_D coming from a Z' boson is governed by $Z'bs$ coupling along with the CKM factor $(V_{us}V^*_{cb})$. Using the allowed range of g^{bs}_L coupling from the current $b \to s$ data, we find that $(\Delta M_D)_{Z'} < 5 \times 10^{-5}\,\text{ps}^{-1}$. A correlation between ΔM_D and ΔM_s is shown in Fig. 3. Thus we see that a possibility of large new physics contributions to ΔM_D coming from a Z' boson is disfavoured by the current measurements in the $b \to s$ sector.

5 Conclusions

In this paper we consider a non-universal Z' model which generates $b \to s\,\mu^+\,\mu^-$ transition at the tree level. Considering the down-type quarks in the quark-doublets to be in the mass-flavour diagonal basis, $u_i \to u_j$ transitions are induced by the up-type quarks mediated by $Z'bs$ and $Z'\mu\mu$ couplings along with suitable combinations of the elements of quark mixing matrix. Thus the current $b \to s$ data is expected to have potential impact on new physics contributions to several observables in the charm sector. Here we study such an impact on decays induced by $c \to u\nu\,\bar{\nu}$ and $c \to u\mu^+\,\mu^-$ transitions along with ΔM_D. Performing a combined fit to $b \to s\,\mu^+\,\mu^-$, ΔM_s and neutrino trident data, we obtain following results:

- The SM predictions of $D^0 \to \pi^0\nu\bar{\nu}$, $D^+ \to \pi^+\nu\bar{\nu}$ and $B_c^+ \to B^+\nu\bar{\nu}$ decays, including the long-distance contributions, are $\sim 10^{-16}$. We find that in Z' models, the branching ratios of these decay can be enhanced by an order of magnitude above their SM values. However this enhancement is not enough to enable the observation of these decay modes in any of the currently running and planned experimental facilities.
- The short distance contribution to the branching ratios of $D^0 \to \mu^+\mu^-$ and $D^+ \to \pi^+\mu^+\mu^-$ are highly suppressed and within SM, these decay modes are dominated by the long-distance effects. The SM branching ratios of $D^0 \to \mu^+\mu^-$ and $D^+ \to \pi^+\mu^+\mu^-$ are $\sim 10^{-11}$ and $\sim 10^{-10}$, respectively. The Z' contribution to the branching ratios of these decays are $\sim 10^{-16}$ and $\sim 10^{-15}$, respectively.
- Within SM, the mixing observable ΔM_D is dominated by long-distance contributions. We find that the Z' boson contribution is restricted to $\sim 10^{-5}\,\text{ps}^{-1}$ which is well below the experimental value.

Thus we conclude that the current data in the B sector puts severe constraints on new physics contributions in semileptonic charm decays and mixing. Any useful enhancement in $c \to u\nu\bar{\nu}$, $c \to u\mu^+\mu^-$ decays and ΔM_D is ruled out in the context of Z' model considered in this work.

Acknowledgements The work of A.K.A. is supported by SERB-India Grant CRG/2020/004576. We would like to thank Shireen Gangal for useful discussions.

Data Availability Statement This manuscript has no associated data or the data will not be deposited. [Authors' comment: This is a theoretical

work. The experimental inputs used in our analysis are in the public domain and we have cited the sources of these inputs in the references.]

Funded by SCOAP[3].

References

1. D. London, J. Matias, arXiv:2110.13270 [hep-ph]
2. R. Aaij, et al. [LHCb], arXiv:2103.11769 [hep-ex]
3. R. Aaij et al. [LHCb], JHEP **08**, 055 (2017). arXiv:1705.05802 [hep-ex]
4. G. Hiller, F. Kruger, Phys. Rev. D **69**, 074020 (2004). arXiv:hep-ph/0310219
5. M. Bordone, G. Isidori, A. Pattori, Eur. Phys. J. C **76**(8), 440 (2016). arXiv:1605.07633 [hep-ph]
6. G. Isidori, S. Nabeebaccus, R. Zwicky, JHEP **12**, 104 (2020). arXiv:2009.00929 [hep-ph]
7. R. Aaij et al. [LHCb], arXiv:2110.09501 [hep-ex]
8. R. Aaij et al. [LHCb Collaboration], Phys. Rev. Lett. **111**, 191801 (2013). arXiv:1308.1707 [hep-ex]
9. R. Aaij et al. [LHCb Collaboration], JHEP **1602**, 104 (2016). arXiv:1512.04442 [hep-ex]
10. S. Descotes-Genon, T. Hurth, J. Matias, J. Virto, JHEP **1305**, 137 (2013). arXiv:1303.5794 [hep-ph]
11. R. Aaij et al. [LHCb Collaboration], JHEP **1509**, 179 (2015). arXiv:1506.08777 [hep-ex]
12. S. Descotes-Genon, J. Matias, J. Virto, Phys. Rev. D **88**, 074002 (2013). arXiv:1307.5683 [hep-ph]
13. W. Altmannshofer, D.M. Straub, Eur. Phys. J. C **73**, 2646 (2013). arXiv:1308.1501 [hep-ph]
14. A.K. Alok, A. Dighe, S. Gangal, D. Kumar, JHEP **06**, 089 (2019). arXiv:1903.09617 [hep-ph]
15. W. Altmannshofer, P. Stangl, arXiv:2103.13370 [hep-ph]
16. A. Carvunis, F. Dettori, S. Gangal, D. Guadagnoli, C. Normand, arXiv:2102.13390 [hep-ph]
17. M. Algueró, B. Capdevila, S. Descotes-Genon, J. Matias, M. Novoa-Brunet, arXiv:2104.08921 [hep-ph]
18. L.S. Geng, B. Grinstein, S. Jäger, S.Y. Li, J. Martin Camalich, R.X. Shi, arXiv:2103.12738 [hep-ph]
19. T. Hurth, F. Mahmoudi, D.M. Santos, S. Neshatpour, arXiv:2104.10058 [hep-ph]
20. A. Angelescu, D. Bečirević, D.A. Faroughy, F. Jaffredo, O. Sumensari, Phys. Rev. D **104**(5), 055017 (2021). arXiv:2103.12504 [hep-ph]
21. Q. Chang, X.Q. Li, Y.D. Yang, JHEP **1004**, 052 (2010). arXiv:1002.2758 [hep-ph]
22. A.J. Buras, J. Girrbach, JHEP **1312**, 009 (2013). arXiv:1309.2466 [hep-ph]
23. Q. Chang, X.Q. Li, Y.D. Yang, J. Phys. G **41**, 105002 (2014). arXiv:1312.1302 [hep-ph]
24. W. Altmannshofer, S. Gori, M. Pospelov, I. Yavin, Phys. Rev. D **89**, 095033 (2014). arXiv:1403.1269 [hep-ph]
25. A. Crivellin, G. D'Ambrosio, J. Heeck, Phys. Rev. D **91**(7), 075006 (2015). arXiv:1503.03477 [hep-ph]
26. D. Aristizabal Sierra, F. Staub, A. Vicente, Phys. Rev. D **92**(1), 015001 (2015). arXiv:1503.06077 [hep-ph]
27. A. Crivellin, L. Hofer, J. Matias, U. Nierste, S. Pokorski, J. Rosiek, Phys. Rev. D **92**(5), 054013 (2015). arXiv:1504.07928 [hep-ph]
28. B. Allanach, F.S. Queiroz, A. Strumia, S. Sun, Phys. Rev. D **93**(5), 055045 (2016). arXiv:1511.07447 [hep-ph]
29. S.M. Boucenna, A. Celis, J. Fuentes-Martin, A. Vicente, J. Virto, Phys. Lett. B **760**, 214 (2016). arXiv:1604.03088 [hep-ph]
30. S.M. Boucenna, A. Celis, J. Fuentes-Martin, A. Vicente, J. Virto, JHEP **1612**, 059 (2016). arXiv:1608.01349 [hep-ph]
31. A. Datta, J. Liao, D. Marfatia, Phys. Lett. B **768**, 265 (2017). arXiv:1702.01099 [hep-ph]
32. L. Darmé, K. Kowalska, L. Roszkowski, E.M. Sessolo, JHEP **1810**, 052 (2018). arXiv:1806.06036 [hep-ph]
33. L. Calibbi, A. Crivellin, F. Kirk, C.A. Manzari, L. Vernazza, Phys. Rev. D **101**(9), 095003 (2020). arXiv:1910.00014 [hep-ph]
34. A. K. Alok, A. Dighe, S. Gangal, J. Kumar, arXiv:2108.05614 [hep-ph]
35. M.K. Mohapatra, N. Rajeev, R. Dutta, arXiv:2108.10106 [hep-ph]
36. A. Crivellin, C.A. Manzari, M. Alguero, J. Matias, Phys. Rev. Lett. **127**(1), 011801 (2021). arXiv:2010.14504 [hep-ph]
37. A.K. Alok, A. Dighe, S. Gangal, D. Kumar, Eur. Phys. J. C **80**(7), 682 (2020). arXiv:1912.02052 [hep-ph]
38. H. Gisbert, M. Golz, D.S. Mitzel, Mod. Phys. Lett. A **36**(04), 2130002 (2021). arXiv:2011.09478 [hep-ph]
39. A.A. Alves Jr. et al. [LHCb], JINST **3**, S08005 (2008)
40. E. Kou et al. [Belle-II], PTEP **2019**(12), 123C01 (2019). arXiv:1808.10567 [hep-ex] [Erratum: PTEP **2020**(2), 029201 (2020)]
41. M. Ablikim et al. [BESIII], Chin. Phys. C **44**(4), 040001 (2020). arXiv:1912.05983 [hep-ex]
42. A. Abada et al. [FCC], Eur. Phys. J. C **79**(6), 474 (2019)
43. A.E. Bondar et al., Charm-Tau Factory. Phys. Atom. Nucl. **76**, 1072–1085 (2013)
44. V. Barger, L. Everett, J. Jiang, P. Langacker, T. Liu, C. Wagner, Phys. Rev. D **80**, 055008 (2009). arXiv:0902.4507 [hep-ph]
45. V. Barger, L.L. Everett, J. Jiang, P. Langacker, T. Liu, C.E.M. Wagner, JHEP **12**, 048 (2009). arXiv:0906.3745 [hep-ph]
46. T. Inami, C.S. Lim, Prog. Theor. Phys. **65**, 297 (1981) [Erratum: Prog. Theor. Phys. **65**, 1772 (1981)]
47. A.J. Buras, M. Jamin, P.H. Weisz, Nucl. Phys. B **347**, 491–536 (1990)
48. L. Di Luzio, M. Kirk, A. Lenz, T. Rauh, JHEP **12**, 009 (2019). arXiv:1909.11087 [hep-ph]
49. A.J. Buras, J. Girrbach-Noe, C. Niehoff, D.M. Straub, JHEP **02**, 184 (2015). arXiv:1409.4557 [hep-ph]
50. A.K. Alok, B. Bhattacharya, D. Kumar, J. Kumar, D. London, S.U. Sankar, Phys. Rev. D **96**(1), 015034 (2017). arXiv:1703.09247 [hep-ph]
51. C. Greub, T. Hurth, M. Misiak, D. Wyler, Phys. Lett. B **382**, 415–420 (1996). arXiv:hep-ph/9603417
52. G. Burdman, E. Golowich, J.L. Hewett, S. Pakvasa, Phys. Rev. D **66**, 014009 (2002). arXiv:hep-ph/0112235
53. S. Fajfer, P. Singer, J. Zupan, Eur. Phys. J. C **27**, 201–218 (2003). arXiv:hep-ph/0209250
54. I. Dorsner, S. Fajfer, J.F. Kamenik, N. Kosnik, Phys. Lett. B **682**, 67–73 (2009). arXiv:0906.5585 [hep-ph]
55. S. de Boer, G. Hiller, Phys. Rev. D **93**(7), 074001 (2016). arXiv:1510.00311 [hep-ph]
56. S. de Boer, B. Müller, D. Seidel, JHEP **08**, 091 (2016). arXiv:1606.05521 [hep-ph]

57. S. Fajfer, N. Košnik, Eur. Phys. J. C **75**(12), 567 (2015). arXiv:1510.00965 [hep-ph]
58. R. Bause, H. Gisbert, M. Golz, G. Hiller, Phys. Rev. D **101**(11), 115006 (2020). arXiv:2004.01206 [hep-ph]
59. Q. Ho-Kim, X.Y. Pham, Phys. Rev. D **61**, 013008 (2000). arXiv:hep-ph/9906235
60. S. Fajfer, S. Prelovsek, Phys. Rev. D **73**, 054026 (2006). arXiv:hep-ph/0511048
61. M. Tanabashi et al. [Particle Data Group], Phys. Rev. D **98**(3), 030001 (2018)
62. A.A. Petrov, Int. J. Mod. Phys. A **21**, 5686–5693 (2006). arXiv:hep-ph/0611361
63. E. Golowich, J. Hewett, S. Pakvasa, A.A. Petrov, Phys. Rev. D **79**, 114030 (2009). arXiv:0903.2830 [hep-ph]
64. S. Aoki et al. [Flavour Lattice Averaging Group], Eur. Phys. J. C **80**(2), 113 (2020). https://doi.org/10.1140/epjc/s10052-019-7354-7. arXiv:1902.08191 [hep-lat]
65. N. Carrasco et al. [ETM], Phys. Rev. D **92**(3), 034516 (2015). arXiv:1505.06639 [hep-lat]
66. E. Golowich, J. Hewett, S. Pakvasa, A.A. Petrov, Phys. Rev. D **76**, 095009 (2007). arXiv:0705.3650 [hep-ph]
67. J. Grygier et al. [Belle], Phys. Rev. D **96**(9), 091101 (2017). arXiv:1702.03224 [hep-ex]
68. O. Lutz et al. [Belle], Phys. Rev. D **87**(11), 111103 (2013). arXiv:1303.3719 [hep-ex]
69. J. Lees et al. [BaBar], Phys. Rev. D **87**(11), 112005 (2013). arXiv:1303.7465 [hep-ex]
70. R. Bause, H. Gisbert, M. Golz, G. Hiller, arXiv:2109.01675 [hep-ph]
71. D.M. Straub, arXiv:1810.08132 [hep-ph]
72. F. James, M. Roos, Comput. Phys. Commun. **10**, 343–367 (1975)
73. S.R. Mishra et al. [CCFR Collaboration], Phys. Rev. Lett. **66**, 3117 (1991)
74. W. Altmannshofer, S. Gori, J. Martín-Albo, A. Sousa, M. Wallbank, arXiv:1902.06765 [hep-ph]
75. R. Bause, H. Gisbert, M. Golz, G. Hiller, arXiv:2007.05001 [hep-ph]
76. R. Bause, H. Gisbert, M. Golz, G. Hiller, Phys. Rev. D **103**(1), 015033 (2021). arXiv:2010.02225 [hep-ph]
77. P. Colangelo, F. De Fazio, F. Loparco, arXiv:2107.07291 [hep-ph]
78. G. Faisel, J.Y. Su, J. Tandean, JHEP **04**, 246 (2021). arXiv:2012.15847 [hep-ph]
79. V. Lubicz et al. [ETM], Phys. Rev. D **96**(5), 054514 (2017). arXiv:1706.03017 [hep-lat] [Erratum: Phys. Rev. D **99**(9), 099902 (2019); Erratum: Phys. Rev. D **100**(7), 079901 (2019)]
80. L.J. Cooper et al. [HPQCD], Phys. Rev. D **102**(1), 014513 (2020). arXiv:2003.00914 [hep-lat] [Erratum: Phys. Rev. D **103**(9), 099901 (2021)]
81. A.A. Petrov, PoS **BEAUTY2016**, 011 (2016). arXiv:1609.04448 [hep-ph]
82. A.A. Petrov, PoS **CKM2016**, 059 (2017). arXiv:1704.03862 [hep-ph]
83. R. Aaij et al. [LHCb], Phys. Lett. B **725**, 15–24 (2013). arXiv:1305.5059 [hep-ex]
84. S. Sahoo, R. Mohanta, Eur. Phys. J. C **77**(5), 344 (2017). arXiv:1705.02251 [hep-ph]
85. R. Aaij et al. [LHCb], Phys. Lett. B **724**, 203–212 (2013). arXiv:1304.6365 [hep-ex]
86. D. Becirevic, A.B. Kaidalov, Phys. Lett. B **478**, 417–423 (2000). arXiv:hep-ph/9904490
87. H. Na, C.T.H. Davies, E. Follana, J. Koponen, G.P. Lepage, J. Shigemitsu, Phys. Rev. D **84**, 114505 (2011). arXiv:1109.1501 [hep-lat]